Published in final edited form as:

Hepatology. 2017 February ; 65(2): 661–677. doi:10.1002/hep.28894.

CD4+ Foxp3+ T cells promote aberrant IgG production and maintain CD8+ T cell suppression during chronic liver disease

Dana Tedesco[1], **Manoj Thapa**[1], **Sanjeev Gumber**[2], **Elizabeth J. Elrod**[1], **Khalidur Rahman**[3], **Chris C. Ibegbu**[1], **Joseph F. Magliocca**[4], **Andrew B. Adams**[4], **Frank Anania**[3], and **Arash Grakoui**[1,5,*]

[1]Emory Vaccine Center, Division of Microbiology and Immunology, Emory University School of Medicine, Atlanta, GA

[2]Division of Pathology and Laboratory Medicine, Emory University School of Medicine, Atlanta, GA

[3]Division of Digestive Diseases, Emory University School of Medicine, Atlanta, GA

[4]Department of Surgery, Emory University School of Medicine, Atlanta, GA

[5]Division of Infectious Disease, Emory University School of Medicine, Atlanta, GA

Abstract

Persistent hepatotropic viral infections are a common etiologic agent of chronic liver disease. Unresolved infection can be attributed to non-functional intrahepatic CD8+ T cell responses. In light of dampened CD8+ T cell responses, liver disease often manifests systemically as Ig-related syndromes due to aberrant B cell functions. These two opposing yet co-existing phenomena implicate the potential of altered CD4+ T cell help. Elevated CD4+ Foxp3+ T cells were evident in both human liver disease and a mouse model of chemically induced liver injury despite marked activation and spontaneous IgG production by intrahepatic B cells. While this population suppressed CD8+ T cell responses, aberrant B cell activities were maintained due to expression of CD40L on a subset of CD4+ Foxp3+ T cells. *In vivo* blockade of CD40L attenuated B cell abnormalities in a mouse model of liver injury. A phenotypically similar population of CD4+ Foxp3+ CD40L+ T cells was found in diseased livers explanted from patients with chronic hepatitis C infection. This population was absent in non-diseased liver tissues and peripheral blood.

Conclusion—Our data indicate that liver disease elicits alterations in the intrahepatic CD4+ T cell compartment that suppress T cell immunity while concomitantly promoting aberrant IgG-mediated manifestations.

Keywords

CD4+Foxp3+T cells; CD40L; B cells; CD8+ T cells; IgG; hepatic fibrosis

*Corresponding Author: Arash Grakoui, Division of Infectious diseases, Emory Vaccine Center, Division of Microbiology and Immunology, Emory University School of Medicine, Atlanta, GA 30322, Telephone: (404) 727-5850; Fax: (404) 727-7768; arash.grakoui@emory.edu.

The authors have no conflicts of interest to disclose.

Hepatic fibrosis can be caused by a wide range of inflammatory insults with chronic viral infections (hepatitis C virus, HCV), alcoholic liver disease (ALD), and non-alcoholic fatty liver diseases (NAFLD) among the most common etiologies (1). Key mediators of fibrotic processes are myeofibroblast-like hepatic stellate cells (HSCs) (2). When provoked, HSCs secrete collagen and extracellular matrix proteins to initiate the tissue wound healing process (1, 3). Once the insult is resolved, fibrosis reverses as healthy tissue eventually replaces scar tissue (1). Persistent or ineffective resolution of fibrosis can lead to irreversible liver injuries such as cirrhosis, hepatocellular carcinoma (HCC) and end-stage liver disease (ESLD) (3). At this stage, the only therapeutic intervention is liver transplantation.

Fibrotic processes can elicit alterations in effector immune responses such as CD4+ T cell and B cell responses (4, 5). Activated HSCs secrete *all-trans* retinoic acid (RA), which promotes and stabilizes CD4+ T cell expression of Foxp3 (5–8). Fibrosis-elicited CD4+Foxp3+ T cells that arise in response to liver insult have been attributed to organ protection from immune-mediated injury in mice (9) and in human patients (5, 6, 10). While this is beneficial for the liver, this population has been implicated in aiding establishment of chronic hepatotropic infections, such as HCV, in human patients by suppressing CD8+ T cell responses (6, 11, 12). Aside from the effects on CD4+ T cell functions, HSC-derived RA can augment B cell survival, plasmablast differentiation and IgG production (4). Aberrant B cell function during liver fibrosis has been linked to systemic manifestations such as hyperglobulinemia, elevated titers of autoimmune anti-nuclear antibody (ANA), and mixed cryoglobulinemia (MC) (reviewed in (13)). The dual effects of fibrotic processes on local suppression of CD8+ T cell responses by accumulation of CD4+Foxp3+T cells with concomitant dysfunctional intrahepatic B cells suggests a potential interplay between fibrosis, CD4+ T cell helper functions and B cells.

Here, we investigated the effects of hepatic fibrosis on the CD4+ T cell compartment and its consequence on the IgG-mediated sequelae of liver disease. Using chemically induced liver injury in mice we found that fibrotic animals demonstrated a CD4+ T cell-dependent increase in serum IgG levels. Despite constitutive intrahepatic B cell production of IgG, there was a liver-specific accumulation of “regulatory” CD4+Foxp3+ T cells during liver injury. Fibrosis-elicited CD4+Foxp3+ T cells effectively suppressed CD8+ T cell responses to cognate antigen while concomitantly permitting B cell activation *in vitro.* Phenotypic analysis demonstrated that a subset of the fibrosis-elicited CD4+Foxp3+ T cell population expressed CD40L and failed to suppress B cell functions *in vitro*. In accordance to our findings in the mouse model, a parallel population and co-incident B cell abnormalities were found in livers explanted from HCV-mediated cirrhotic patients. Taken together, our data suggests that fibrosis drives accumulation of intrahepatic CD4+Foxp3+ T cells that regulate CD8+ T cell responses and promote extrahepatic symptoms of disease.

Materials and Methods

Animals

Six to eight week-old C57BL6/J males, C57BL6/J-Tg (TcraTcrb)1100Mjb/J (OT-I) and Foxp3^{GFP} mice were purchased from Jackson Laboratories (Bar Harbor, ME) and housed in the specific pathogen-free Emory University Vivarium in compliance with the Institutional

Animal Care and Use Committee (IACUC) and NIH guidelines for the care and use of laboratory animals.

Human subjects

A total of 22 patients undergoing orthotopic liver transplantation (n=16), or non-HCV, non-ALD, non-NAFLD related liver re-sectioning ("non-fibrotic control tissue", n=6) at Emory Transplant Center of Emory University Hospital were enrolled in the study in accordance with the Emory University Institutional Review Board (IRB) approval (IRB# 00006248). Patient characteristics with clinical information and relevant biological variables are summarized in Supplementary Tables 2 and 3. Written informed consent was obtained from each patient and IRB #00006248 conforms to the guidelines of the 1975 Declaration of Helsinki (revised 2013).

Carbon tetrachloride (CCl_4)-treatment

Mice were injected with CCl_4 (0.5 μg/g of body weight, Sigma) intra-peritoneally (I.P.) mixed with olive oil in 1:10 ratio. Control animals were given olive oil alone. Treatments were administered every 3 days for a total of 12 treatments; animals were sacrificed per IACUC guidelines within one day following final treatment. For CD4 depletion studies, 0.5 mg CD4 depleting antibody (clone GK1.5) was administered I.P. on day -1 and 0 and every 14 days thereafter during CCl_4-treatment. Where applicable, 250 μg anti-CD154 (CD40L, clone MR1) was administered I.P. on day −1 and 0, or 2 or 3 weeks into CCl_4-treatment regimen. Antibody was given every three days thereafter.

Isolation of liver cell populations

Animals were sacrificed as per IACUC guidelines, and livers were perfused with 1X PBS (Lonza, Switzerland) and harvested. Tissues were processed by enzymatic digestion with 2mg/mL type IV collagenase (Worthington, NY) in serum-free media DMEM-F12 (Lonza). Following incubation, tissue digests were strained through sterile cheesecloth to remove particulate matter, and enzymatic reaction was quenched with complete media. Liver lymphocytes were isolated by Percoll or Ficoll-paque (GE, Sweden) gradients. CD4+ T cells were isolated by negative selection (STEM CELL). Where applicable, further positive selection of CD4+CD25+ T cells was performed using anti-CD25 PE (BD Biosciences) and anti-PE Microbeads (Miltenyi Biotec, CA). B cells were isolated using CD19-positive selection kit for both mouse and human studies (Miltenyi). Purity and composition was assessed on a BD LSRII Custom order system. Human liver interstitial mononuclear cell (LIMC) were isolated as described (14).

Analysis of HSCs activation

HSCs were enriched as described previously (5). Cell suspensions were blocked in FACS Buffer (0.5% FCS, 0.01% Sodium azide, 1X PBS) supplemented with 10% normal mouse serum (Sigma) and anti-CD16/32 (2.4G2) then stained for CD45.2 (104; Tonbo Biosciences, CA). Dead cells were excluded using standard staining procedures for live/dead with Ghost Dye 780 (Tonbo) and fixed with BD Cytofix/Cytoperm (BD Biosciences) according to manufacturer's instructions. To determine activation, intracellular α-SMA-PE (R&D

systems) was stained at room temperature. HSCs were acquired on a FACSAria II equipped with a UV laser (355nm) (BD Biosciences) and were defined as UV auto-fluorescent positive and CD45-negative populations as indicated in Supplemental Figure S1C. Auto-fluorescence and debris were excluded using a 405nm laser (450/50BP).

Histology and Immunohistochemistry

Following perfusion, liver sections were immediately fixed in 10% formalin for 24 hours, and transferred to 70% ethanol and paraffin embedded. Standard Sirius Red and H&E staining were performed in the Pathology Core of Emory Vaccine Center. Fibrosis was quantified as described (15), histopathological findings are summarized in Supplementary Table 1.

Alanine amino-transferase assay

Serum was sampled immediately following animal sacrifice. Levels of alanine amino-transferase (ALT) were detected by standard procedures by the Yerkes Molecular Pathology Core of the Emory Vaccine Center.

Flow cytometry analysis

For mouse studies, cells were blocked as described. The following fluorochrome-conjugated antibodies were purchased from Tonbo Biosciences; anti-CD3 (17A2), CD4 (RM4-5), CD8 (53–6.7), CD25 (PC.61), B220 (RA3-6B2), CD44 (IM7), CD45.2 (104), CD19 (1D3). Anti-CD69 (H1.2F3) was purchased from eBioscience. Anti-ICOS (C398.4A), FasL (MFL3), IgD (11–26c.2a), CD11b (M1/70) and PD-1 (29F-1A12) were purchased from Biolegend. CD95 (Jo2) was purchased from BD biosciences. Where applicable, cells were pre-incubated with biotinylated anti-mouse CXCR5 (clone 2G8, BD Biosciences) for 1 hour at room temperature, or FasL for 30 minutes at room temperature then followed by either streptavidin-APC or -PE (Invitrogen) and surface markers. Dead cells were excluded with Ghost Dye-780 (Tonbo). Cells were fixed and permeabilized per manufacturer's instructions (Transcription Factor Staining Set; Tonbo) then intracellular stained for Foxp3 (3G3; Tonbo), CD40L (MR1; BD Biosciences), and/or Ki-67 (B56; BD Biosciences). For studies using Annexin-V/Propidium Iodide (PI), staining was performed per manufacturer's recommendation (BD) and acquired immediately. For human studies, thawed cryopreserved cell suspensions blocked in FACS Buffer containing anti-human CD32 (Miltenyi) and 10% human serum type AB (Sigma). Cells were subsequently stained with relevant antibodies as described: anti-CD3 (OKT3), CD4 (OKT4), CD25 (BC96) (Tonbo). Anti-FoxP3 (259D), CXCR5 (J252D4), ICOS (C398.4A) and PD-1 (EH12.2H7) were purchased from Biolegend. Anti-CD40L (CD154, TRAP-1) was purchased from BD biosciences. All samples were acquired within 24 hours on a BD LSRII Custom Order system. In all FACS experiments, auto-fluorescence and debris were excluded using a 407nm laser (525/40BP 475LP); gates were determined using appropriate isotype and/or fluorescence minus one control. FACS data were analyzed with FlowJo version 9.6.4 (Tree Star, Inc.).

ELISPOT

Milipore multiscreen-IP plates (Milipore, MA) were prepared per manufacturer's instruction and coated with appropriate antibodies in PBS: 2ug/mL Goat Anti-Mouse Ig (Southern Biotech), or 4–8ug/mL anti-human IgG (Rockland Biosciences, NY). The following day, plates were washed and blocked with complete medium. Bulk cell suspensions were prepared, diluted appropriately and incubated in complete IMDM (10% FCS, 1.0% Pen/Strep) for 18 hours at 37°C and 5% CO_2. Standard ELISPOT procedures were followed using biotinylated anti-mouse IgG (Sigma) or anti-Human IgG (mABtech) followed by streptavidin-ALP (mABTech). Assay was developed with NBT/BCIP Substrate (ThermoScientific) and analyzed using CTL Immunospot 5.0 software (Cellular Tech Ltd). Data were calculated as antibody-secreting (ASC) spots/10^6 lymphocytes.

Serum Ig ELISA

Nunc Maxi-sorp plates (Thermo-scientific, USA) were coated with 1ug/mL anti-mouse Ig (Southern Biotech) overnight at 4°C. Goat-anti mouse IgG-HRP was used for detection of IgG (Southern Biotech, USA). BD OPT-EIA kit was used for detection (BD Biosciences, USA). Standard curves were generated using known concentrations of mouse IgG.

Co-culture assays

CD19+ B cells (2.5×10^5) isolated from naïve C57BL6/J spleen were co-cultured in duplicate with indicated purified CD4+ T cells (1.25×10^5) pooled from either control liver, CCl_4-treated liver, control spleen, or B cells alone in the presence of complete IMDM alone or supplemented with 2.0ug/mL LPS (Sigma) for 5 days at 37°C and 5% CO_2. Following incubation, ELISPOT assay was performed as described earlier. FACS for B cell activation was performed (Live B220+CD44+Ki-67+). Where applicable, CD4+Foxp3^{GFP} T cells were used to sort indicated subsets, and cultured with B cells at a 2:1 ratio (B cells: CD4+Foxp3+) as described previously.

CD8+ T cell suppression assay

Splenic CD8+ T cells were purified (Miltenyi) from transgenic mice specific for ovalbumin residues 257–264 (SIINFEKL) (OT-I) and labeled with 5uM CFSE (Biolegend). The CD8-depleted fraction was irradiated (3000rad) and pulsed for one hour with 3ug/mL SIINFEKL at 37°C. Purified CD4+CD25+ T cells derived from indicated organs were cultured in 1:1 ratio with CD8+ T cells (1×10^5). Unloaded or SIINFEKL-loaded stimulator cells were added to cultures in a 1:5 ratio (stimulators: CD8). Cultures were incubated for five days at 37°C and 5.0% CO_2. IFNγ in the supernatant was detected via ELISA (BD Biosciences). Cells were stained appropriately for FACS and acquired immediately on a BD LSRII custom order system. Analysis was performed on live, non-autofluorescent, CD8+ T cells expressing the indicated markers.

HEp-2 ANA assay

HEp-2 substrate slides (Antibodies, Inc.) were used for the detection of ANA titers in mouse serum as per manufacturer's recommendations. For mouse studies, secondary anti-IgG FITC (Jackson Immunotech), and for human studies, anti-IgG FITC (Antibodies, Inc.) was used.

Bead enriched CD19+ human lymphocytes were seeded at 5×10^4 per well in the presence of complete IMDM alone or supplemented with 1ug/mL R848 (Invivogen) and 20U/mL rhIL-2 (Roche) and cultured for 5 days at 37°C with 5% CO_2. Supernatants were harvested for detection of ANA-positive IgG and cells were analyzed by ELISPOT.

Statistical analysis

Statistical analyses were performed using Prism5 software (GraphPad) using a two-tailed Mann-Whitney *U* test, one-way ANOVA or two-tailed Spearman correlation. Statistical significance was considered *p<0.05, **p<0.005, ***p<0.0005.

Results

Aberrant IgG-production during hepatic fibrosis requires CD4+ T cells

In this study, our aim was to determine the role of CD4+ T cells in aberrant B cell IgG production during liver disease. We found that mice undergoing CCl_4-treatment exhibited characteristic hepatic parenchyma with periportal bridging fibrosis as measured by Sirius red and H&E staining (Fig. 1A). Animals demonstrated an elevated serum ALT level consistent with liver injury (Fig. 1B). CCl_4-treated animals demonstrated a three-fold increase in circulating serum IgG in comparison to oil-treated control animals (Fig. 1C). Antibody-mediated (clone GK1.5) CD4+ T cell depletion during liver injury markedly reduced serum IgG levels, despite comparable collagen deposition as measured by Sirius red staining, serum ALT and severity of fibrosis lesions (average score 3) (Fig. 1A–C, Supplementary Fig. S1A, B & Supplementary Table 1). Consistent with this finding, FACS analysis of enriched HSC expression of α-smooth muscle actin (α-SMA), an activation marker, was indistinguishable in CD4-intact versus CD4-depleted fibrotic animals (Fig. S1C, D). Collectively, these data indicate that CCl_4-elicited fibrosis does not require CD4+ T cells; this is in agreement with a previous report (16). Despite comparable indicators of hepatic injury, CD4+ T cell depletion substantially reduced the spontaneous IgG production in the livers of fibrotic animals as detected by direct *ex vivo* ELISPOT analysis of intrahepatic B cells (Fig. 1D). In contrast, B cells from CD4-intact fibrotic livers constitutively produced IgG in the absence of any stimulation (Fig. 1D). This phenomenon was not apparent in splenic B cells (Fig. S2A, B). Importantly, serum from CCl_4-treated fibrotic mice demonstrated elevated ANA IgG titers (titers 200), which was not detected in control animals and CD4-depleted fibrotic animals (titers <50) (Fig. 1E). Combined together, our data suggest that CD4+ T cells are required for aberrant intrahepatic IgG-production during liver fibrosis.

Fibrosis-elicited CD4+Foxp3+ T cells do not suppress B cell activity

Fibrotic processes such as RA production by HSCs have been shown to promote CD4+ T cell expression of Foxp3 and enhance regulatory function (5, 8, 9). We found a liver-specific accumulation of CD4+Foxp3+ T cells following CCl_4-treatment with an increased frequency (15.05 ± 3.8%) in comparison to oil-treated controls (3.15 ± 1.3%). This was not observed in the spleen (Fig. 2A). Surprisingly, despite increased frequency of “regulatory” phenotype CD4+ T cells, spontaneous IgG production was still evident by fibrotic liver B cells (Fig. 1). Phenotypic analysis of these intrahepatic B cells reveals a heightened activation state, with

an increased frequency of the IgD- CD95+ (Fas) population co-expressing activation markers CD44 and Ki-67 (Fig. S3A). In line with this observation and in accordance with our previous study, fibrotic liver B cells demonstrated enhanced survival by *ex vivo* Annexin-V/PI analysis (Fig. S3B) (4). Thus, B cell activation co-exists with a marked increase of CD4+Foxp3+ T cells during hepatic fibrosis.

To investigate this dichotomy, enriched CD4+CD25+ T cells (>80% expressed Foxp3, Fig. S4A) from the livers and spleens of oil- or CCl_4-treated mice were co-cultured with CD19-enriched splenic B cells in presence of LPS stimulation (1:2 CD4: B cell ratio) (Fig. S4A). B cells in co-culture with splenic and control liver-derived CD4+CD25+ T cells markedly reduced this IgG production (260 ± 55.0 IgG+ and 250 ± 155.2 IgG+ ASC/10^6, respectively) (Fig. 2B). However, CD4+CD25+ T cells derived from fibrotic livers did not inhibit IgG production by B cells (1100 ± 45.1 IgG+ASC/10^6). Likewise, co-culture with fibrotic liver-derived CD4+CD25+ T cells did not suppress the B cell activation (CD44 and Ki-67 expression on Live, B220+ cells) compared to splenic and control liver CD4+CD25+ T cell co-cultures (Fig. 2C). The same result was observed in experiments were performed with “untouched” B cells (data not shown). We also investigated the effect of fibrosis on the CD25-negative fraction of CD4+ T cells. Under the same co-culture conditions, all CD4+CD25-negative T cells had a comparable effect on B cell activation (Fig. S4, B–D). Thus, these findings suggest that fibrotic liver disease promotes altered CD4+Foxp3+ T: B cell interaction.

Fibrosis-elicited CD4+Foxp3+ T cells suppress CD8+ T cell responses

Chronic liver disease presents a unique dichotomy of Ig-mediated extrahepatic symptoms and heightened B cell activation (13, 17, 18) that co-exist with intrahepatic immunosuppresive milieu characterized by increased frequencies of CD4+Foxp3+ T cells (5–7, 9, 11). Our own findings are consistent with these B cell-mediated sequelae of disease (Fig. 2). Therefore, we aimed to interrogate the suppressive activity of the fibrosis-induced CD4+Foxp3+ T cells on CD8+ T cell activation by cognate antigen in the mouse model. To test this hypothesis, we performed parallel co-culture experiments with CD4+CD25+ T cells (>80% Foxp3+) isolated from spleen, control and fibrotic livers and cultured with CFSE-labeled OT-I CD8+ T cells in the presence of OVA (257–264)-pulsed stimulator cells. After five days of culture, CD4+Foxp3+ T cells comparably reduced CD8+ T cell proliferation, irrespective of their origin (Fig. 3A). In line with this observation, CD8+ T cells cultured with CD4+Foxp3+ T cells expressed similar levels of activation markers, CD25 and CD44 (Fig. 3A). Furthermore, analysis of culture supernatants indicated that all isolated CD4+Foxp3+ T cells significantly suppressed IFNγ production by responding OT-I CD8+ T cells (Fig. 3B). These data demonstrate that fibrosis-elicited CD4+Foxp3+ T cells regulate CD8+ T cell responses to the same extent as non-fibrotic liver and their splenic counterparts. Thus, our observations suggest that CD4+Foxp3+ T cells induced by liver injury selectively regulate CD8+ T cell responses while simultaneously permitting B cell activation and IgG production.

Fibrotic liver CD4+Foxp3+ T cells up-regulate CD40L, CD69 and PD-1 expression

Co-existence of B cell activation and abundance of CD4+Foxp3+ T cells with regulatory capacity on CD8+ T cells during fibrotic liver disease may be indicative of altered CD4+ T cell help to B cells. As such, we investigated the effects of fibrosis on the CD4+ T cell compartment by FACS analysis to identify co-expression of Foxp3 with markers that may potentiate B cell activation. We found augmented expression of PD-1, an activation marker implicated immune-modulatory functions(19, 20)); CD69, an activation marker (21); and CD40L (CD154), a molecule critical for IgG-class switching (22), on CD4+Foxp3+ T cells from fibrotic livers (Fig. 4A, frequencies represent Foxp3+ population). This phenotype was not observed in oil-treated control livers (Fig. 4A) or spleens (Fig. S5A, B). Although fibrotic liver CD4+ Foxp3- T cells increased CD69 and PD-1 expression, there was no overt consequence of this activation state with respect to B cell function (Fig. S4, B-D). Therefore, liver-specific accumulation of CD4+Foxp3+ T cells during fibrosis represents a heterogeneous population with elevated expression of CD40L, CD69 and PD-1.

With respect to Ig-related syndromes in human liver disease patients, ectopic lymphoid structures have been identified in livers from patients with chronic HCV (23–25). As such, we performed FACS analysis for the presence of T follicular helper (Tfh) or regulatory (Tfr) CD4+ T cells in fibrotic mouse livers using canonical follicular helper markers, CXCR5 and ICOS (23, 26). Although an accumulation of CD4+CXCR5+ICOS+ T cells was observed in both Foxp3+ and Foxp3 negative compartments of CD4+ T cells in fibrotic livers, the frequency of CD4+CXCR5+ICOS+ T cells was significantly increased within Foxp3+ compartment (Fig. 4B). However, there was no apparent consequence of the two-fold increase of CD4+ Foxp3-negative Tfh-phenotype with respect to B cell activation *in vitro* (Fig. S4, B–D).

CD40L expression is localized to CD4+Foxp3+ CXCR5− ICOS− T cells

To further determine the significance of CXCR5 and ICOS expressions on B cell IgG production, we performed co-cultures with FACS-purified CXCR5+ICOSdim/+ (canonical Tfr), CXCR5−ICOS+, and CXCR5−ICOS−CD4+Foxp3+ T cells from transgenic mice that express green fluorescent protein (GFP)-Foxp3 (Fig. 5A). CD4+Foxp3+ cells expressing CXCR5+ICOS+ and CXCR5−ICOS+ isolated from spleen, oil and fibrotic livers comparably suppressed B cell IgG production in response to LPS (Fig. 5B–C). Although the CXCR5−ICOS− population derived from spleen and oil-treated livers inhibited IgG production, fibrotic liver CXCR5−ICOS− population permitted LPS-mediated IgG production (Fig. 5D). Parallel FACS analysis further indicated that CD40L expression predominantly localizes to this population of CD4+Foxp3+ T cells obtained fibrotic livers that are CXCR5−ICOS− (Fig. 5E). Thus, our observations indicate that fibrosis drives accumulation of CD4+Foxp3+ T cells with varying B cell regulatory functions dictated by CD40L expression.

In vivo CD40L blockade during liver injury attenuates IgG aberrations

Interestingly, a previous report identified CD40L expression in total RNA isolated from livers of HCV patients suffering from aberrant Ig-related syndromes (18). Our own findings pinpoint CD40L expression exclusively on CD4+Foxp3+ T cells during liver disease (Fig.

4A). CD40L-mediated CD4+ T cell help promotes B cell activation and facilitates fine-tuning of immune responses (21, 22) and may implicate this signaling pathway to extrahepatic symptoms of liver disease. To test this hypothesis, we performed antibody-mediated CD40L (clone MR1) blockade prior to ("Day-1"), or during ("Week 2", "Week 3") the course of CCl_4-treatment (Fig. 6A). Blockade of CD40L signaling before and during CCl_4 treatment regimen attenuated IgG production by intrahepatic B cells (Fig. 6B). This corresponded to a significant reduction in total serum IgG (Fig. 6C). Pre-treatment of animals with anti-CD40L resulted in ANA-IgG that was indistinguishable from control animals (titers <50)(Fig. 6D). Interestingly, later introduction of anti-CD40L treatment (Week 2 and Week 3 groups) attenuated ANA titers (titers 100–200) in comparison to CCl_4-treated animals (titers >400) (Fig. 6D). This may be the result of *in vivo* stability of IgG, which has a reported half-life of approximately 21 days (27). Thus, CD40L blockade may be sufficient to halt production at the level of intrahepatic B cell IgG (Fig. 6B); ANA-IgG produced before blockade may persist in circulation (Fig. 6D). These data implicate CD40L expression, which is primarily localized to CD4+Foxp3+ T cells, is critical for aberrant IgG-production during liver disease.

Accumulation of CD4+Foxp3+CD40L+ T cells in explanted HCV patient livers

Next, phenotypic analysis was performed on CD4+Foxp3+ T cells from explanted livers of HCV-infected cirrhotic patients based on canonical follicular helper markers, CXCR5, ICOS, and CD40L expression. Clinical characteristics of explanted cirrhotic livers derived from HCV infected patients and "non-fibrotic control" tissues obtained from donors undergoing surgical re-sectioning for non-HCV, non-NAFLD, non-ALD related medical treatment are summarized in Supplementary Tables 2 and 3. In accordance with our findings in the mouse model, there was a liver-specific increase in CD4+Foxp3+CD25+T cells from HCV explants (n=16, 12.81±5.20%) compared to non-fibrotic controls (n=6, 3.22±1.04%) (Fig. 7A). This finding was consistent with previous reports of increased frequency of CD4+Foxp3+ T cells in livers of patients infected with HCV (6, 7, 11). Alterations in frequency were not noticed in peripheral blood derived from control or HCV subjects (control subjects n=6, 5.00±1.61%; HCV donors n=6, 6.08±1.24%, $p>0.05$) despite a marked increase observed in HCV patient-matched livers at the same time of transplantation (Fig. 7A). Furthermore, we found increased PD-1 (55.75±16.5%, n=9) and CD40L (14.86±7.08%, n=9) expression in intrahepatic CD4+Foxp3+ T cells from chronic HCV patients compared to non-fibrotic controls (34.30±9.08%, $p<0.02$, n=6, and 0.50±1.00%, $p<0.005$, n=4, respectively) (Fig. 7B). Similar to the mouse CCl_4-model of fibrosis, CD40L expression on CD4+Foxp3+ T cells was also predominantly restricted to the subset that lacked canonical follicular helper markers CXCR5 and ICOS (Fig. 7C).

Aberrant IgG production correlates with frequency of CD4+Foxp3+ T cells in explanted HCV patient livers

Next, we determined whether liver-specific accumulation of CD4+Foxp3+T cells modulates IgG production in chronic HCV patients. In agreement with the murine model, intrahepatic B cells from livers explanted from HCV-infected individuals demonstrated constitutive IgG production in the absence of any stimulation (Fig. 8A). This was not observed from peripheral blood or non-fibrotic control intrahepatic B cells (Fig. 8A). Interestingly,

supernatants from cultured B cells isolated from HCV patient livers were positive for ANA-IgG titers independent of stimulation with R848 and IL-2 (Fig. 8B). R848 and IL-2 stimulation was chosen as human intrahepatic B cells are hypofunctional to LPS, due to very low expression of TLR4 (28). Intrahepatic B cell spontaneous IgG production in HCV patient livers significantly correlated with the frequency of CD4+Foxp3+ T cells (Fig. 8C). Surprisingly, both parameters were independent of patient viremia (Fig. S6). Taken together, characteristics of CD4+Foxp3+ T cells and B cell IgG-mediated aberrations in explanted cirrhotic livers from HCV human patients parallel those in the murine CCl_4-model. Thus, fibrotic liver disease elicits a population of CD4+Foxp3+CD40L+ T cells that promote extrahepatic manifestations of liver disease via aberrant intrahepatic IgG production.

Discussion

Inflammatory conditions and environmental factors can highly influence CD4+Foxp3+ T cell plasticity and result in various pathology-associated sub-populations; classified as “reprogrammed” Tregs, or “Ex-Tregs” (29). Treg “reprogramming” has been implicated as providing early co-stimulatory signals that promote anti-tumor CTL immunity during vaccination and tumor challenges (21). Induction of this population is reliant on the presence of interleukin-6 (IL-6), and MHCII+ antigen presenting cells (21), both of which are understood to be abundant in the fibrotic liver microenvironment (5, 8). Alternatively, elegant fate mapping and epigenetic studies have indicated that spatial localization of CD4+Foxp3+ T cells can influence *Foxp3* stability and regulatory functions (30); in this context this population is termed “ex-Treg”, as this inflammatory population arises from peripheral CD4+Foxp3+ T cells which transiently up-regulate Foxp3. Foxp3 down-regulation or loss of expression has been associated with inflammatory functions (31, 32).

Furthermore, other correlates of liver fibrosis such as complement proteins (33) have also been implicated in CD4+ T cell differentiation into a unique population of CD4+Foxp3+ T cells (34, 35). Stimulation of human PBMC through the complement receptor can result in a unique “Treg” population that expresses CD40L amongst other co-stimulatory markers that can permit dendritic cell maturation, suppress effector T cell responses, and interact with B cells to promote Ig-production (34, 35). Combined together, these findings delineate key factors surrounding CD4+Foxp3+ T cell-mediated regulatory versus pathogenic functions during specific disease or inflammatory states. To our knowledge, none of these populations have been investigated during liver disease, thus there is a limited understanding of the relationship between the fibrotic liver microenvironment and effect on origin(s) and functional plasticity of CD4+Foxp3+ T cells. Therefore, we cannot conclusively categorize these CD4+Foxp3+ T cells accumulated in the fibrotic livers despite some of the shared traits associated with various disease-related pathogenic Tregs.

In light of the protective role CD4+Foxp3+ T cells play in the maintenance of the hepatic microenvironment and limiting immune-mediated injury to the liver (9, 10), we have identified a key contribution of the CD40L+ sub-population to extrahepatic manifestations of aberrant B cell functions (Fig. 5). This finding is consistent with immunologic characteristics of chronic HCV infection in the clinic: ineffective anti-viral CD8+ T cell responses (6, 10–12, 36) that co-exist with B cell abnormalities (13, 17, 18, 23, 24).

Differential mechanisms of regulation by CD4+Foxp3+ T cells may shed light on this dichotomy. Phenotypically, the bulk CD4+Foxp3+ T cell population demonstrates high levels of PD-1 expression (Fig. 4). PD-1 signaling is implicated in suppression of CD8+ T cell functions and exhaustion; both of which contribute to chronic viral infections (37). In contrast, PD-1 expression on CD4+ T cells in B cell follicles has been attributed to modulating the quality and quantity of long-lived plasma cell pool (19, 20). With regard to B cell modulatory markers, our own data draws particular attention to CD40L signaling that arises primarily in fibrotic liver derived intrahepatic CD4+Foxp3+ T cells (Fig. 4). Due to the role in Ig-class switching (22), but insignificant influence on CD8+ T cell responses to viral infections (38), CD40L expression may account for contradictory functions of total enriched CD4+CD25+ T cells that suppress CD8+ T cells (Fig. 3) yet promote B cell activation when sourced from fibrotic livers (Fig. 2). In line with this hypothesis, *in vitro* isolation of the CD40L-expressing subset (Fig. 5) and *in vivo* blockade of CD40L in the mouse model of liver injury (Fig. 6) suggest that this population critically contributes to extrahepatic IgG aberrations.

Although therapeutic potential of anti-CD40L treatment has been realized for treatment of autoimmune conditions (39), its introduction into clinical practice had significant adverse events due to Fc-recognition of the antibody(40) (41). Recent development of Fc-deficient CD40L blockade antibody has achieved the same therapeutic benefits as earlier biologics without complications of its predecessors in pre-clinical trials (42). Our data suggest that such strategies may benefit management of Ig-related sequelae of chronic liver disease (Fig. 6).

Localization of IgG production and CD40L expressing CD4+Foxp3+ T cells to the liver, but not the periphery has important implications when considering novel “Treg” transfer therapies to promote liver repair (43). The microenvironment in which the “Treg” enters may have critical influence on what types of functions it can promote. This is certainly a consideration in the case of the liver microenvironment during fibrosis or other ongoing inflammatory events. Thus, liver fibrosis highlights a scenario in which accumulation of regulatory-phenotype T cells may propagate adverse autoantibody mediated pathology, rather than promote tolerance.

The current work demonstrates that chemically induced liver injury in mice can recapitulate both CD4+Foxp3+ CD40L+ T cell phenotype and constitutive intrahepatic IgG production found in explanted livers from cirrhotic patients infected with HCV. Together, these observations imply that shared mechanisms of post-insult hepatic tissue repair govern liver CD4+ T cell phenotype and function. As a result, fibrosis-induced alterations to the intrahepatic CD4+ T cell compartment are not only critical for IgG-anomalies, but also ineffective CD8+ T cell responses associated with chronic liver disease. Decoupling extrahepatic manifestations from the etiologic agent opens up novel avenues for potential therapeutic management of chronic liver disease.

Supplementary Material

Refer to Web version on PubMed Central for supplementary material.

Acknowledgments

This project was supported by NIH grants R01AI070101, R01AI124680, and R01AI126890 to A.G., R01 DK062092 and VA I01BX001746 to F.A.A., and ORIP/OD P51OD011132 (formerly NCRR P51RR000165) to the Yerkes National Primate Research Center. M.T. is supported by National Institute of Diabetes, Digestive and Kidney Diseases (NIDDK) NRSA Fellowship (F32DK101163). This work was facilitated by the Immunology and Flow Cytometry Core of the Center for AIDS Research at Emory University (P30AI050409). Its contents are solely the responsibility of the authors and do not necessarily represent the official views of the NIH.

We are grateful to the donors and their families of the Emory Transplant Center for invaluable consented participation in this study. We thank the Emory Transplant center team: surgical and nursing staff, coordinators, Shine Thomas for their assistance and cooperation. We thank Victoria M. Velazquez, J. Brett Mendel, Young-Jin Seo and Aryn Price for critical reading of the manuscript and fruitful scientific discussions. We thank Kiran Gill and Barbara Cervasi of the Emory Vaccine Center Flow Cytometry and Pathology Cores for technical assistance throughout the study.

List of abbreviations

HCV	Hepatitis C
RA	*all-trans* retinoic acid
ANA	anti-nuclear antibodies
CCl_4	carbon tetrachloride
HSC	hepatic stellate cell
Ig	immunoglobulin
IgG	immunoglobulin G
IFNγ	interferon gamma
GFP	green fluorescent protein
LPS	lipopolysaccharide

References

1. Pellicoro A, Ramachandran P, Iredale JP, Fallowfield JA. Liver fibrosis and repair: immune regulation of wound healing in a solid organ. Nat Rev Immunol. 2014; 14:181–194. [PubMed: 24566915]
2. Mederacke I, Hsu CC, Troeger JS, Huebener P, Mu X, Dapito DH, Pradere J-P, et al. Fate tracing reveals hepatic stellate cells as dominant contributors to liver fibrosis independent of its aetiology. Nature Communications. 2013; 4:2823.
3. Yin C, Evason KJ, Asahina K, Stainier DY. Hepatic stellate cells in liver development, regeneration, and cancer. J Clin Invest. 2013; 123:1902–1910. [PubMed: 23635788]
4. Thapa M, Chinnadurai R, Velazquez VM, Tedesco D, Elrod E, Han JH, Sharma P, et al. Liver fibrosis occurs through dysregulation of MyD88-dependent innate B-cell activity. Hepatology. 2015; 61:2067–2079. [PubMed: 25711908]
5. Dunham RM, Thapa M, Velazquez VM, Elrod EJ, Denning TL, Pulendran B, Grakoui A. Hepatic stellate cells preferentially induce Foxp3+ regulatory T cells by production of retinoic acid. Journal of Immunology. 2013; 190:2009–2016.
6. Claassen MA, de Knegt RJ, Tilanus HW, Janssen HL, Boonstra A. Abundant numbers of regulatory T cells localize to the liver of chronic hepatitis C infected patients and limit the extent of fibrosis. J Hepatol. 2010; 52:315–321. [PubMed: 20129690]

7. Lan RY, Cheng C, Lian ZX, Tsuneyama K, Yang GX, Moritoki Y, Chuang YH, et al. Liver-targeted and peripheral blood alterations of regulatory T cells in primary biliary cirrhosis. Hepatology. 2006; 43:729–737. [PubMed: 16557534]
8. Ichikawa S, Mucida D, Tyznik AJ, Kronenberg M, Cheroutre H. Hepatic stellate cells function as regulatory bystanders. Journal of Immunology. 2011; 186:5549–5555.
9. Stross L, Günther J, Gasteiger G, Asen T, Graf S, Aichler M, Esposito I, et al. Foxp3+ regulatory T cells protect the liver from immune damage and compromise virus control during acute experimental hepatitis B virus infection in mice. Hepatology. 2012; 56:873–883. [PubMed: 22487943]
10. Lohse AW, Weiler-Normann C, Tiegs G. Immune-mediated liver injury. J Hepatol. 2010; 52:136–144. [PubMed: 19913936]
11. Franceschini D, Paroli M, Francavilla V, Videtta M, Morrone S, Labbadia G, Cerino A, et al. PD-L1 negatively regulates CD4+CD25+Foxp3+ Tregs by limiting STAT-5 phosphorylation in patients chronically infected with HCV. J Clin Invest. 2009; 119:551–564. [PubMed: 19229109]
12. Boettler T, Spangenberg HC, Neumann-Haefelin C, Panther E, Urbani S, Ferrari C, Blum HE, et al. T Cells with a CD4+ CD25+ regulatory phenotype suppress in vitro proliferation of virus-specific CD8+ T cells during chronic hepatitis C virus infection. Journal of virology. 2005; 79:7860–7867. [PubMed: 15919940]
13. Chi ZC, Ma SZ. Rheumatologic manifestations of hepatic diseases. Hepatobiliary Pancreatic Disease Int. 2003; 2:32–37.
14. Velazquez VM, Uebelhoer LS, Thapa M, Ibegbu CC, Courtney C, Bosinger SE, Magliocca JF, et al. Systems biological analyses reveal the hepatitis C virus (HCV)-specific regulation of hematopoietic development. Hepatology. 2015; 61:843–856. [PubMed: 25331524]
15. Ishak K, Baptista A, Bianchi L, Callea F, De Groote J, Gudat F, Denk H, et al. Histological grading and staging of chronic hepatitis. J Hepatol. 1995; 22:696–699. [PubMed: 7560864]
16. Novobrantseva TI, Majeau GR, Amatucci A, Kogan S, Brenner I, Casola S, Shlomchik MJ, et al. Attenuated liver fibrosis in the absence of B cells. J Clin Invest. 2005; 115:3072–3082. [PubMed: 16276416]
17. Pyrsopoulos NT, Reddy KR. Extrahepatic manifestations of chronic viral hepatitis. Curr Gastroenterol Rep. 2001; 3:71–78. [PubMed: 11177698]
18. Mayo MJ, Mosby JM, Jeyarajah R, Combes B, Khilnani S, Al-Halimi M, Handem I, et al. The relationship between hepatic immunoglobulin production and CD154 expression in chronic liver diseases. Liver International. 2006; 26:187–196. [PubMed: 16448457]
19. Good-Jacobson KL, Szumilas CG, Chen L, Sharpe AH, Tomayko MM, Shlomchik MJ. PD-1 regulates germinal center B cell survival and the formation and affinity of long-lived plasma cells. Nature immunology. 2010; 11:535–542. [PubMed: 20453843]
20. Linterman MA, Pierson W, Lee SK, Kallies A, Kawamoto S, Rayner TF, Srivastava M, et al. Foxp3+ follicular regulatory T cells control the germinal center response. Nat Med. 2011; 17:975–982. [PubMed: 21785433]
21. Sharma MD, Hou D-y, Baban B, Koni PA, He Y, Chandler PR, Blazar BR, et al. Reprogrammed Foxp3 + Regulatory T Cells Provide Essential Help to Support Cross-presentation and CD8 + T Cell Priming in Naive Mice. Immunity. 2010; 33:942–954. [PubMed: 21145762]
22. Crotty S. A brief history of T cell help to B cells. Nat Rev Immunol. 2015; 15:185–189. [PubMed: 25677493]
23. Racanelli V, Sansonno D, Piccoli C, D'Amore FP, Tucci F, Dammacco F. Molecular characterization of B cell clonal expansions in the liver of chronically hepatitis C virus-infected patients. Journal of Immunology. 2001; 167:21–29.
24. Racanelli V, Rehermann B. The liver as an immunological organ. Hepatology. 2006; 43:S54–62. [PubMed: 16447271]
25. Pitzalis C, Jones GW, Bombardieri M, Jones SA. Ectopic lymphoid-like structures in infection, cancer and autoimmunity. Nature Rev Immunol. 2014; 14:447–462. [PubMed: 24948366]
26. Murakami J, Shimizu Y, Kashii Y, Kato T, Minemura M, Okada K, Nambu S, et al. Functional B-cell response in intrahepatic lymphoid follicles in chronic hepatitis C. Hepatology. 1999; 30:143–150. [PubMed: 10385650]

27. Vidarsson G, Dekkers G, Rispens T. IgG subclasses and allotypes: from structure to effector functions. Front Immunol. 2014; 5:520. [PubMed: 25368619]
28. Vaure C, Liu Y. A comparative review of toll-like receptor 4 expression and functionality in different animal species. Front Immunol. 2014; 5:316. [PubMed: 25071777]
29. Guo J, Zhou X. Regulatory T cells turn pathogenic. Cellular and Molecular Immunology. 2015; 12:525–532. [PubMed: 25942597]
30. Miyao T, Floess S, Setoguchi R, Luche H, Fehling HJ, Waldmann H, Huehn J, et al. Plasticity of Foxp3(+) T cells reflects promiscuous Foxp3 expression in conventional T cells but not reprogramming of regulatory T cells. Immunity. 2012; 36:262–275. [PubMed: 22326580]
31. Zheng Y, Rudensky AY. Foxp3 in control of the regulatory T cell lineage. Nat Immunol. 2007; 8:457–462. [PubMed: 17440451]
32. Williams LM, Rudensky AY. Maintenance of the Foxp3-dependent developmental program in mature regulatory T cells requires continued expression of Foxp3. Nat Immunol. 2007; 8:277–284. [PubMed: 17220892]
33. Hillebrandt S, Wasmuth HE, Weiskirchen R, Hellerbrand C, Keppeler H, Werth A, Schirin-Sokhan R, et al. Complement factor 5 is a quantitative trait gene that modifies liver fibrogenesis in mice and humans. Nature genetics. 2005; 37:835–843. [PubMed: 15995705]
34. Fuchs A, Atkinson JP, Fremeaux-Bacchi V, Kemper C. CD46-induced human Treg enhance B-cell responses. European Journal of Immunology. 2009; 39:3097–3109. [PubMed: 19784949]
35. Barchet W, Price JD, Cella M, Colonna M, MacMillan SK, Cobb JP, Thompson PA, et al. Complement-induced regulatory T cells suppress T-cell responses but allow for dendritic-cell maturation. Blood. 2006; 107:1497–1504. [PubMed: 16239430]
36. Shoukry NH, Cawthon AG, Walker CM. Cell-mediated immunity and the outcome of hepatitis C virus infection. Annual review of microbiology. 2004; 58:391–424.
37. Wherry EJ, Kurachi M. Molecular and cellular insights into T cell exhaustion. Nature Reviews Immunology. 2015; 15:486–499.
38. Whitmire JK, Slifka MK, Grewal IS, Flavell RA, Ahmed R, Whitmire JK, Slifka MK, et al. CD40 ligand-deficient mice generate a normal primary cytotoxic T-lymphocyte response but a defective humoral response to a viral infection. Journal of Virology. 1996:70.
39. Kalled SL, Cutler AH, Datta SK, Thomas DW. Anti-CD40 ligand antibody treatment of SNF1 mice with established nephritis: preservation of kidney function. J Immunol. 1998; 160:2158–2165. [PubMed: 9498753]
40. Kawai T, Andrews D, Colvin RB, Sachs DH, Cosimi AB. Thromboembolic complications after treatment with monoclonal antibody against CD40 ligand. Nat Med. 2000; 6:114.
41. Robles-Carrillo L, Meyer T, Hatfield M, Desai H, Davila M, Langer F, Amaya M, et al. Anti-CD40L immune complexes potently activate platelets in vitro and cause thrombosis in FCGR2A transgenic mice. J Immunol. 2010; 185:1577–1583. [PubMed: 20585032]
42. Shock A, Burkly L, Wakefield I, Peters C, Garber E, Ferrant J, Taylor FR, et al. CDP7657, an anti-CD40L antibody lacking an Fc domain, inhibits CD40L-dependent immune responses without thrombotic complications: an in vivo study. Arthritis Res Ther. 2015; 17:234. [PubMed: 26335795]
43. Oo YH, Sakaguchi S. Regulatory T-cell directed therapies in liver diseases. J Hepatol. 2013; 59:1127–1134. [PubMed: 23727305]

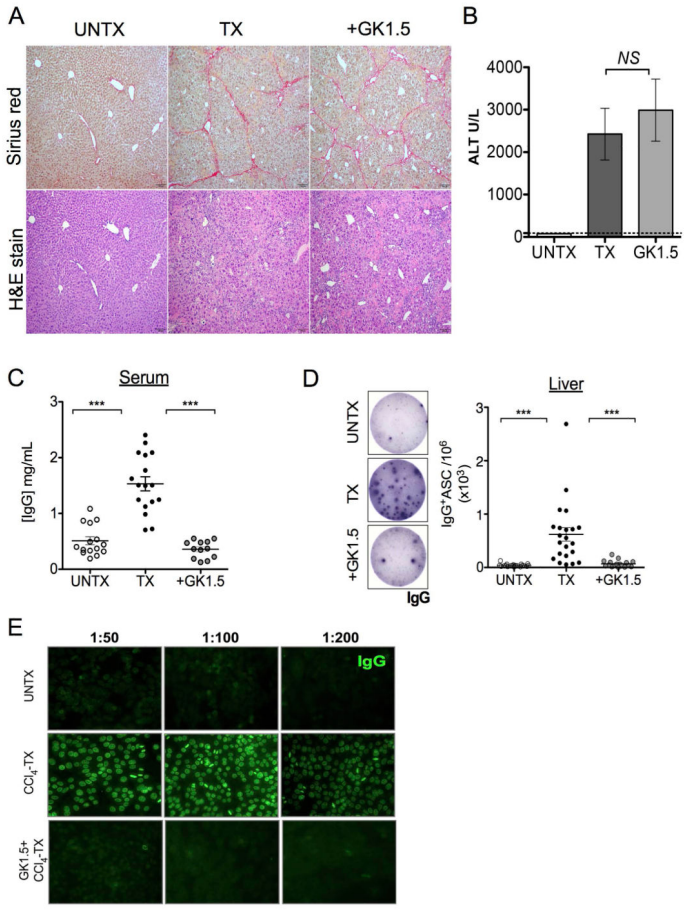

FIGURE 1. Aberrant IgG-production during hepatic fibrosis requires CD4+ T cells

C57BL6/J mice were treated with CCl_4 three times per week for a total of 12 treatments to induce liver fibrosis. (**A**) Following treatment, liver tissues were harvested from oil-treated control (UNTX), CCl_4-treated (TX), and CCl_4 plus GK1.5 monoclonal antibody-treated (+GK1.5) mice and processed for histological analyses by Sirius red and H&E staining (magnification 100x). Data are representative of 2 independent experiments (n=5 mice per group). Serum samples were collected from these mice and analyzed for (**B**) ALT levels and (**C**) IgG titers by using a limiting dilution standard IgG ELISA. Graph plot shown is representative of 3 independent experiments (n=3–5 per group). (**D**) Bulk liver lymphocytes isolated from UNTX, TX and +GK1.5 mice were cultured in complete IMDM medium for 18–20 hrs in presence of 5.0% CO_2 at 37^0C, and analyzed for IgG production by e*x vivo* IgG ELISPOT method. (**E**) Serum samples (dilution as indicated) were analyzed for ANA-IgG titers by using a standard HEp-2 substrate staining with anti-mouse IgG FITC. Data shown is representative of 3 independent experiments (n=3–5 mice per group). ***p<0.0005, two-tailed Mann-Whitney *U* test.

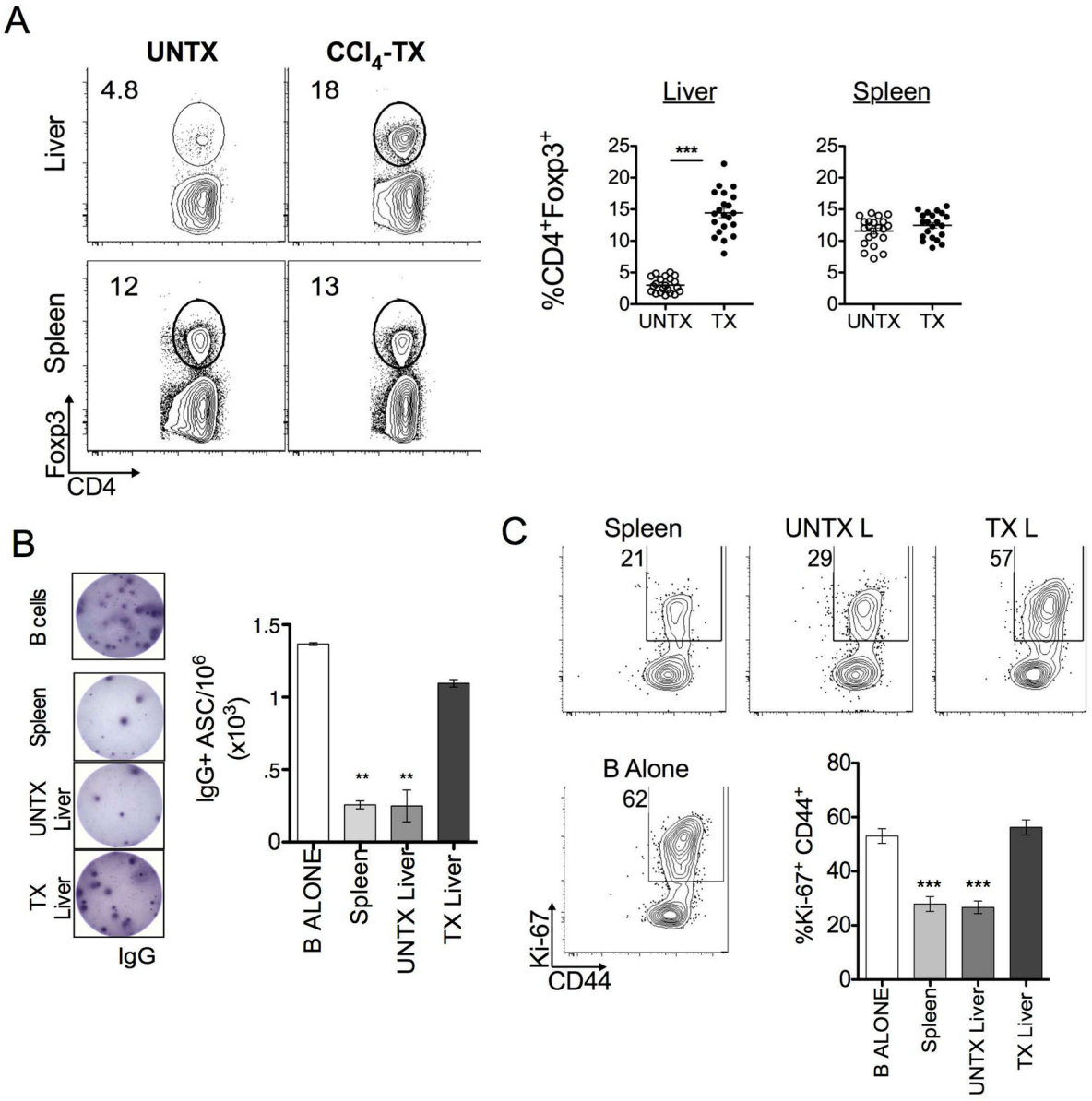

FIGURE 2. Fibrosis-elicited CD4+Foxp3+ T cells do not suppress B cell activity

(**A**) Control (UNTX) and CCl_4-treated (TX) mice were harvested and processed for phenotypic analysis of CD4+Foxp3+ T cells by FACS. FACS plots are representative of 3 independent experiments (n=3–5 mice per group). Frequencies represent the Live, Non-autofluorescent, CD3+ CD4+Foxp3+ T cell gate. (**B**) ELISPOT analysis of B cell co-culture alone or in a 2:1 ratio with CD25-enriched CD4+ T cells in the presence of LPS stimulation for 5 days. The number of IgG producing cells per million (1×10^6) was calculated as described, each well was plated in duplicate and manually counted under a microscope. Representative of 5 independent experiments, isolated from pooled lymphocytes (n=3–5 mice per group) is shown. (**C**) Frequency of B220+ Ki-67+ CD44+ B cells co-cultured as indicated in the presence of LPS stimulation for 5 days. Statistics were calculated relative to

culture of B cells alone using a two-tailed Mann-Whitney *U* Test (***p<0.0005, **p<0.005, *p<0.05). Error bars represent SEM.

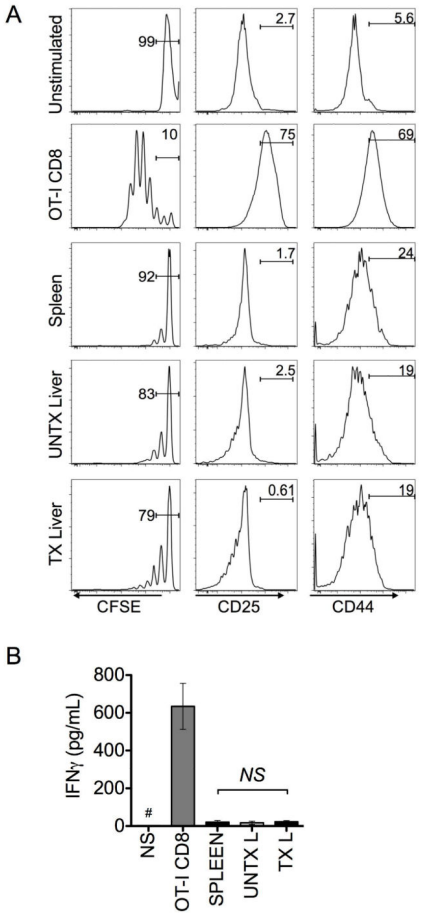

FIGURE 3. Fibrotic liver CD4+Foxp3+ T cells suppress CD8+ T cell response

(**A)** CFSE labeled OT-I CD8+ T cells were cultured in the presence of irradiated CD8-depleted splenocytes pulsed with 3ug/mL ovalbumin peptide (SIINFEKL) 257–264 or unloaded (5:1 ratio, CD8: stimulators). CD4+CD25+ T cells (>80% Foxp3+) were added from indicated sources in a 1:1 ratio with CD8+ T cells. After 5 days of culture, proliferation was assed by CFSE dilution on live, non-auto-fluorescent CD8+ T cells, (**left)**. Activation was assessed by CD25 and CD44 expression (**middle and right)**. (**B)** ELISA was performed on supernatants to quantify IFN**γ** production from indicated wells (# denotes IFN**γ** concentration below 15pg/mL in supernatant). Data are representative of 3 independent experiments with pooled CD4+CD25+ T cells from indicated organs (n=3–5 animals per group). Statistics were calculated using one-way ANOVA of duplicate wells from at least 3 independent experiments (*$p<0.05$); error bars reflect SEM.

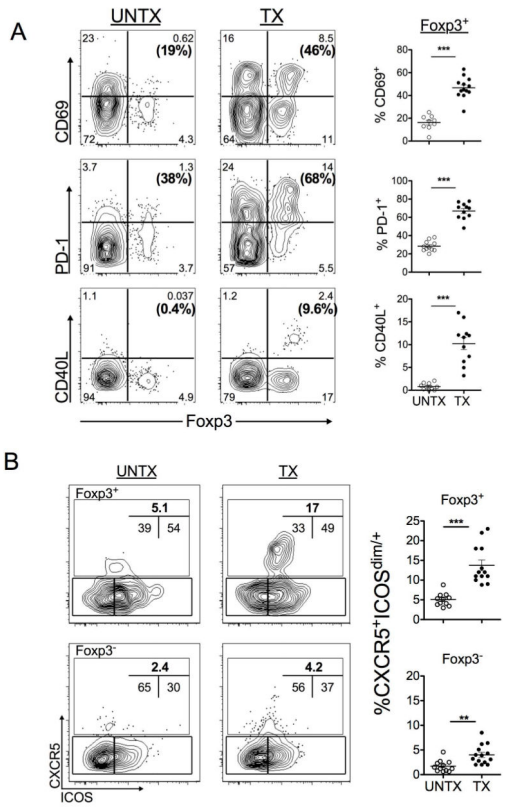

FIGURE 4. Fibrotic liver CD4+Foxp3+ T cells up-regulate CD69, PD-1 and CD40L expression

(**A**) FACS analysis of phenotypic changes in the total live, non-autofluorescent hepatic CD4+ T cell compartment following course of CCl_4-treatment. Frequencies (bold) reflect the proportion of CD4+Foxp3+ T cells expressing the specified marker. Gates were defined based on appropriate fluorescent minus one controls. FACS plots are representative of at least 3 independent experiments (n=3–5 mice per group). (**B)** FACS analysis of CD4+Foxp3+ T cells from control liver (UNTX) and fibrotic livers (TX) based on follicular helper markers CXCR5 and ICOS expression is shown. Cells were gated on live, non-autofluorescent CD4+ T cells and indicated Foxp3 expression. FACS plot shown is representative of 3 independent experiments (n=3–5 mice per group). Statistics were calculated using a two-tailed Mann-Whitney *U* Test (***p<0.0005, **p<0.005, *p<0.05).

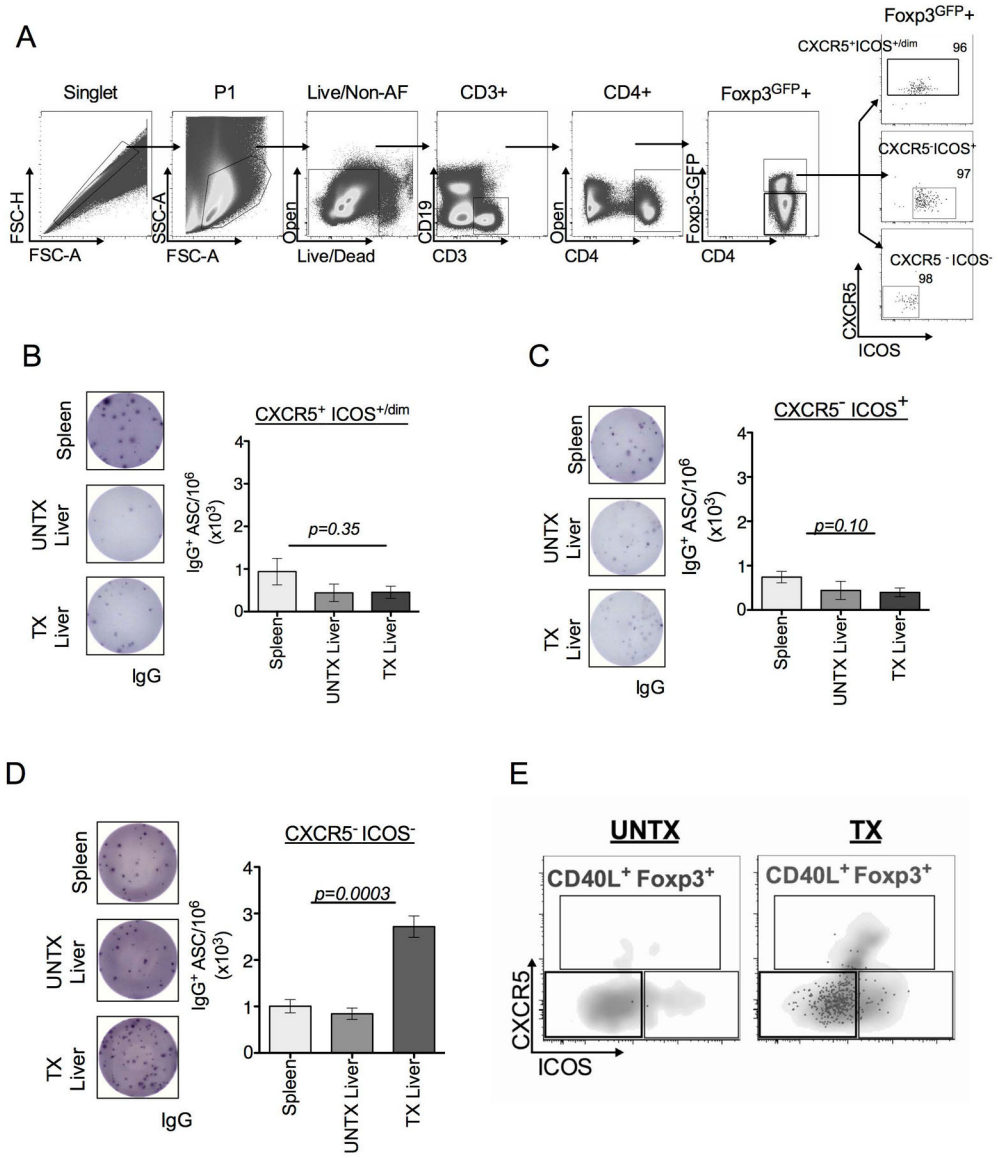

FIGURE 5. CD40L is primarily expressed on CXCR5 and ICOS double negative CD4+Foxp3+ T cells

(**A**) Transgenic mice that express GFP-Foxp3 were treated with CCl_4 to induce hepatic fibrosis. CD4+ (GFP-Foxp3+) T cells were sorted based on expression of CXCR5 and ICOS into three populations: CXCR5+ ICOSdim/+ (**B**), CXCR5- ICOS+ (**C**), or CXCR5- ICOS- (**D**) by FACS. Post-sort purity of splenic, untreated liver, and fibrotic liver populations was >95% (**A, far right,** representative of indicated CD4+Foxp3^{GFP}+ subsets). Sort strategy represented is from fibrotic liver lymphocytes. Sorted cells CXCR5+ ICOSdim/+ (**B**), CXCR5-ICOS+ (**C**), or CXCR5-ICOS- (**D**) CD4+Foxp3+T cells from indicated organs were co-cultured with CD19-enriched B cells in ratio of 1:2 (CD4: B cells) for 5 days in the presence of 2ug/mL LPS stimulation and subsequently analyzed for IgG production by ELISPOT. (**E)** FACS plots showing CD40L expression in CD4+Foxp3+ CXCR5- ICOS- T cell compartment in fibrotic (TX) livers in comparison to absence of this population in non-

fibrotic (UNTX) livers. Gray density plot represents the total CD4+Foxp3+T cell compartment, black overlay dots represent the CD40L+ population of CD4+Foxp3+ T cells. All data are representative of 3 independent experiments with sorted cell populations pooled from 3–5 animals per group. Statistical significance was determined by one-way ANOVA of duplicate wells of three independent experiments (data represented in **B–D,** ***$p<0.0003$) Error bars represent SEM.

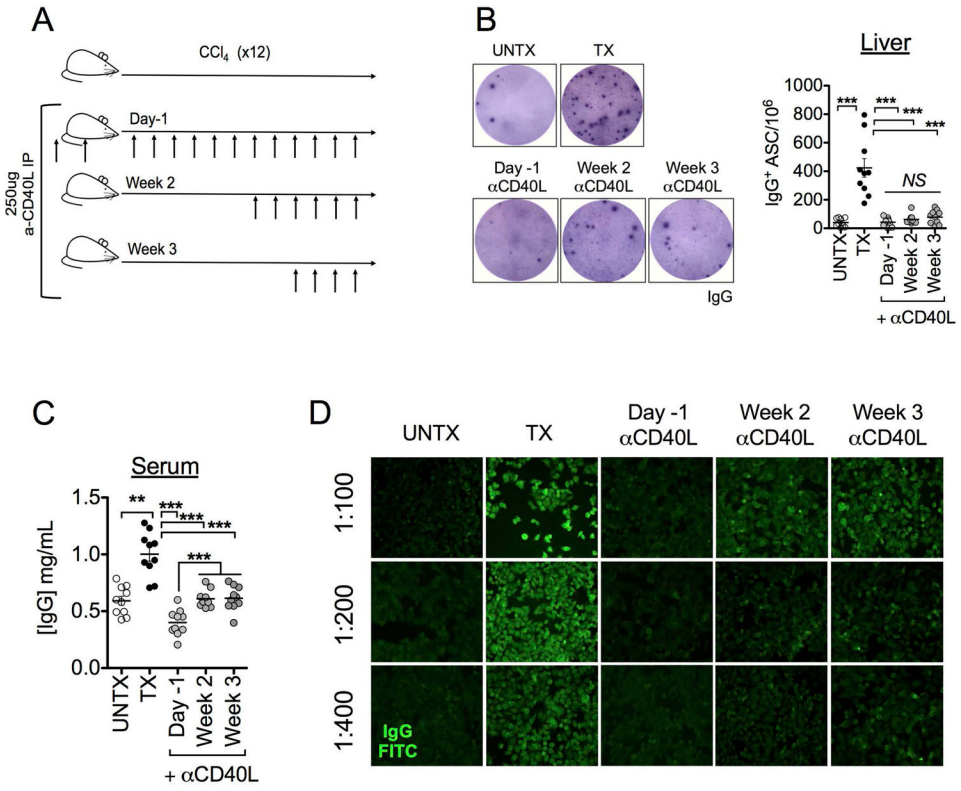

FIGURE 6. ***In vivo*** **blockade of CD40L attenuates Ig-mediated manifestations of liver fibrosis**

(**A**) Animals were treated I.P. with 250 μg hamster anti-Mouse CD40L one day prior to and upon initiation of CCl_4-treatment ("Day-1"), or begun 2 weeks ("Week 2") or 3 weeks ("Week 3") into CCl_4 regimen and every three days thereafter; antibody administrations are indicated by arrows (**B**) *Ex vivo* ELISPOT of intrahepatic B cell production of IgG in untreated (UNTX), CCl_4 treated (TX), and α-CD40L-treated groups cultured overnight in media alone. (**C**) Serum IgG and (**D**) ANA IgG titers are attenuated when CD40L is blocked during fibrosis. Data are representative of 2 independent experiments (n=5 animals per group). Statistical significance was determined by a two-tailed Mann Whitney *U* test (***p<0.0005, ** p<0.005).

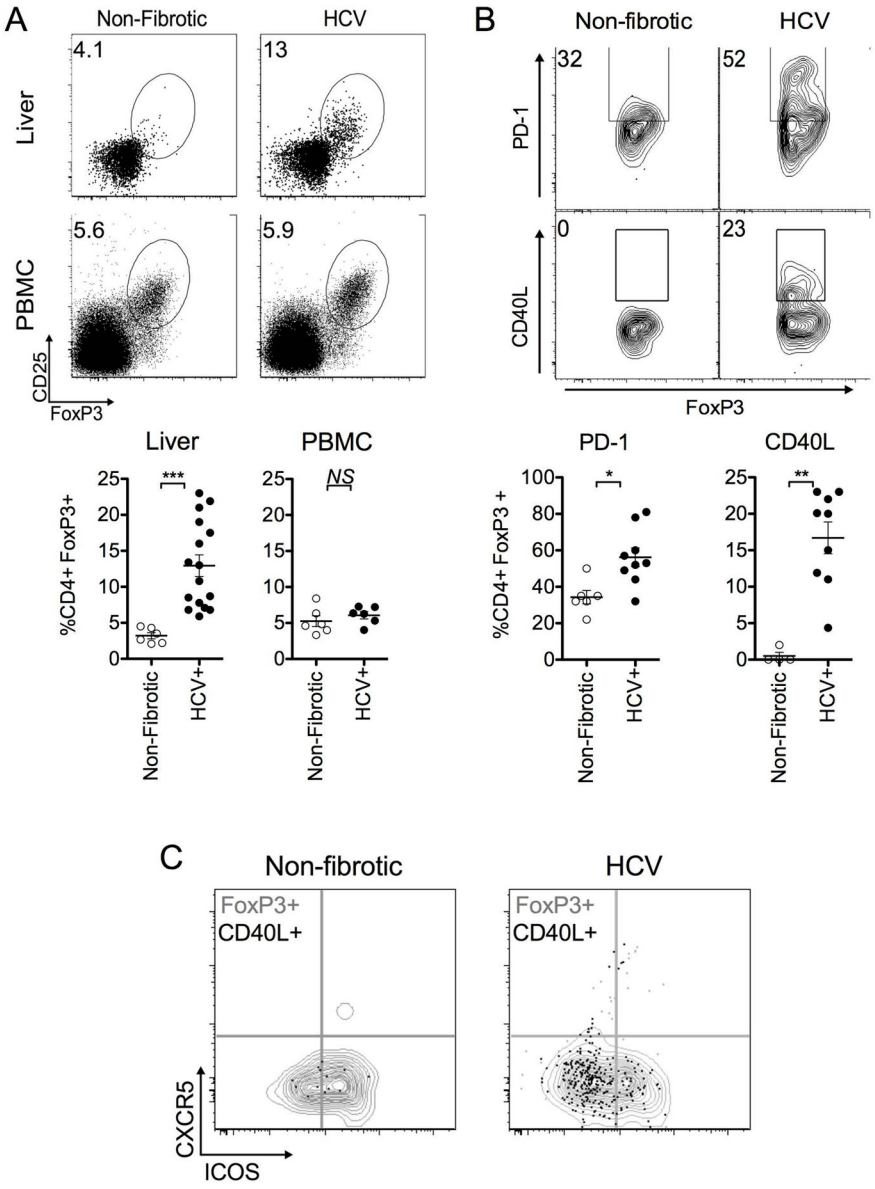

FIGURE 7. Phenotypic analysis of CD4+Foxp3+ T cells in explanted livers from HCV patients

(**A**) FACS analysis of cryopreserved livers explanted from cirrhotic HCV human patients (n=16) or patients undergoing non-HCV, non-NASH, non-ALD related surgical re-sectioning (“non-fibrotic control” n=6) (top) and PBMC (control donors, n=6, HCV, matched to livers at time of transplantation n=6), (bottom) based on expression of FoxP3 and CD25. Frequencies were determined by gating on live, non-autofluorescent CD4+ T cells co-expressing CD25 and FoxP3. (**B**) FACS analysis of cryopreserved HCV explanted (n=9) or non-fibrotic control liver (n=4–6) based on CD4+Foxp3+ T cell gated expression of PD-1 and CD40L. (**C**) CD4+Foxp3+ CD40L+ T cells from livers explanted from HCV patients predominantly localize to the CXCR5- ICOS- population. Gray contour plot represents the total CD4+Foxp3+T cell compartment, while black dot overlay represents the CD4+Foxp3+ CD40L+ T cell population. Data are representative of n=9 HCV patients, and n=4 “non-

fibrotic control" patients. All statistical analyses (unless otherwise indicated) were calculated by a two-tailed Mann-Whitney *U* test (***p<0.0005, **p<0.005, *p<0.05).

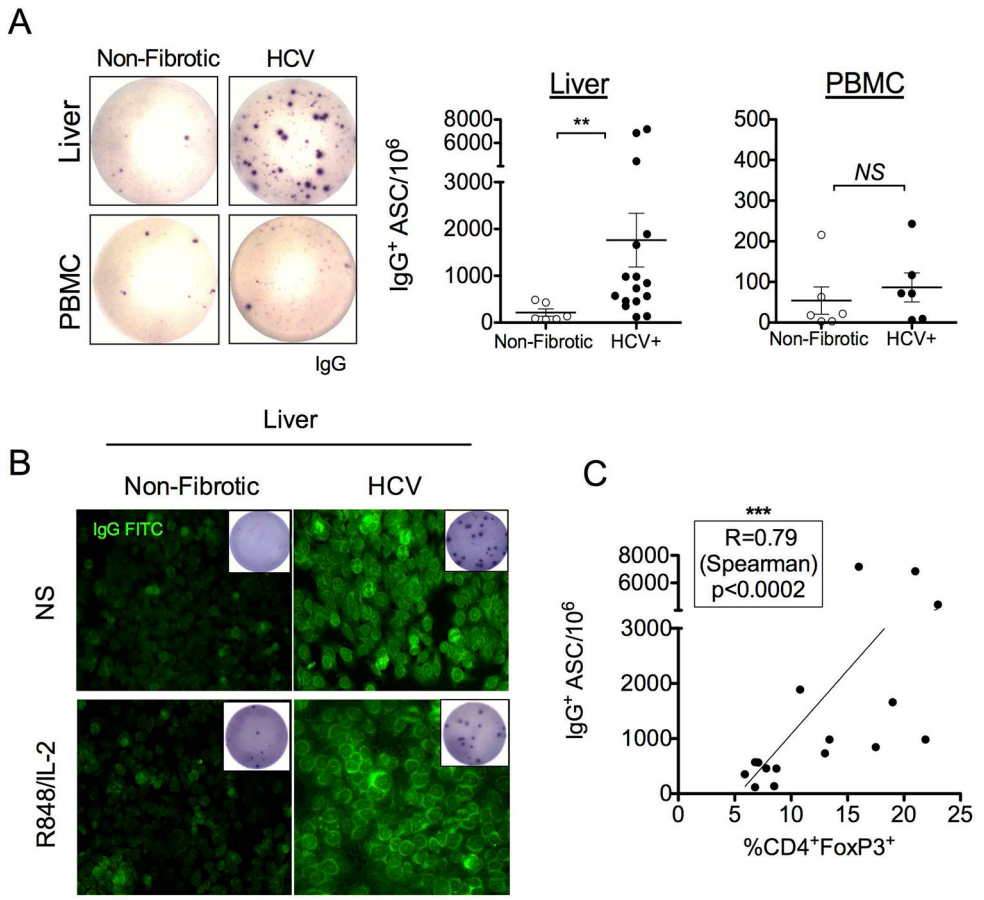

FIGURE 8. Aberrant IgG production correlates with frequency of CD4+Foxp3+ T cells in explanted HCV patient livers

(**A**) Spontaneous IgG ELISPOT of cryopreserved non-fibrotic control (n=6) and HCV (n=16) liver lymphocytes (top), or peripheral blood (control subjects, n=6, patient matched HCV, n=6, bottom) lymphocytes, cultured in complete IMDM for 16–18h in 5.0% CO_2 and 37^0C without any stimulation. (**B**) Supernatants of cultured purified intrahepatic B cells from HCV patients have detectable ANA-IgG. Representative images of culture supernatant incubated with HEp-2 ANA substrate and counterstained with anti-IgG FITC. IgG ELISPOT of bead enriched CD19+ B cells ($5.0x10^4$/well) from non-fibrotic control tissue (n=3) or HCV (n=6) livers after 5 days of culture in IMDM alone or with R848 (1ug/mL) and IL-2 (20U/mL) stimulation was performed to determine the presence of ASC (inset). (**C**) The frequency of intrahepatic CD4+Foxp3+ T cells correlates with spontaneous IgG production in explanted HCV livers (n=16) (Spearman R=0.79, ***p<0.0002, two-tailed).